Solar Phys (2018) 293:59
https://doi.org/10.1007/s11207-018-1286-5

# Meridional Motions and Reynolds Stress Determined by Using Kanzelhöhe Drawings and White Light Solar Images from 1964 to 2016

**Domagoj Ruždjak**[1] · **Davor Sudar**[1] · **Roman Brajša**[1] · **Ivica Skokić**[1] · **Ivana Poljančić Beljan**[2] · **Rajka Jurdana-Šepić**[2] · **Arnold Hanslmeier**[3] · **Astrid Veronig**[3,4] · **Werner Pötzi**[4]

Received: 5 October 2017 / Accepted: 18 March 2018 / Published online: 30 March 2018

**Abstract** Sunspot position data obtained from Kanzelhöhe Observatory for Solar and Environmental Research (KSO) sunspot drawings and white light images in the period 1964 to 2016 were used to calculate the rotational and meridional velocities of the solar plasma. Velocities were calculated from daily shifts of sunspot groups and an iterative process of calculation of the differential rotation profiles was used to discard outliers. We found a differential rotation profile and meridional motions in agreement with previous studies using sunspots as tracers and conclude that the quality of the KSO data is appropriate for analysis of solar velocity patterns. By analyzing the correlation and covariance of meridional velocities and rotation rate residuals we found that the angular momentum is transported towards the solar equator. The magnitude and latitudinal dependence of the horizontal component of the Reynolds stress tensor calculated is sufficient to maintain the observed solar differential rotation profile. Therefore, our results confirm that the Reynolds stress is the dominant mechanism responsible for transport of angular momentum towards the solar equator.

**Keywords** Sunspots · Differential rotation · Velocity fields

## 1. Introduction

Precise determination of solar large-scale velocity patterns can provide information about the transport of angular momentum in the solar convective zone and provide important observational constraints for solar dynamo models. One possibility to determine the solar velocity field is by observing the motions of structures which can be observed at the surface of

---

✉ D. Ruždjak
rdomagoj@geof.hr

[1] Hvar Observatory, Faculty of Geodesy, University of Zagreb, Kačićeva 26, 10000 Zagreb, Croatia

[2] Department of Physics, University of Rijeka, Radmile Matejčić 2, 51000 Rijeka, Croatia

[3] IGAM – Institute of Physics, University of Graz, Universitätplatz 5, 8010 Graz, Austria

[4] Kanzelhöhe Observatory for Solar and Environmental Research, Kanzelhöhe 19, 9521 Treffen am Ossiacher See, Austria

the Sun. Most often sunspots and sunspot groups were used as tracers (*e.g.* Howard, Gilman, and Gilman, 1984; Balthasar, Vazquez, and Wöhl, 1986; Howard, 1991; Lustig and Wöhl, 1994; Pulkkinen and Tuominen, 1998a; Wöhl and Brajša, 2001; Zuccarello and Zappalá, 2003; Sudar *et al.*, 2014; Sivaraman *et al.*, 2010; Mandal *et al.*, 2017; Sudar *et al.*, 2017, among many others). Besides tracing sunspots, other methods have been used for assessment of solar large-scale flows, for instance: Doppler measurements (*e.g.* Hathaway, 1996) and tracing coronal bright points (CBP) (*e.g.* Sudar *et al.*, 2016). In recent years the observations of solar velocity field were revolutionized by helioseismology (Hanasoge *et al.*, 2015). While all mentioned methods give very similar results for solar rotation, the obtained results for meridional flows are controversial, as described in Hathaway (1996) and Sudar *et al.* (2017). The Doppler measurements as well as observation and analysis of global oscillations reveal that there is a poleward meridional circulation in the near surface layers of the Sun in both hemispheres. This is in agreement with the results of most theoretical models which predict unicellular meridional circulation directed poleward at the top and equatorward at the bottom of the convection zone (Brun and Rempel, 2009). Observations utilizing tracers show more complicated patterns of meridional flows. All kinds of meridional flow directions were found (poleward, equatorward, towards and away from the center of activity). However, the results for meridional circulation using tracers are influenced by several effects. First, the active regions locally modify the amplitude and direction of meridional circulation (Haber *et al.*, 2004; Švanda, Kosovichev, and Zhao, 2008). Next, the movement of the (magnetic) tracers do not represent the movement of the solar surface plasma, but the movement of the layer where the observed features are anchored, which might change with time (Ruždjak *et al.*, 2004), and finally, the solar meridional circulation might be variable, as pointed out by Hathaway (1996).

Differential rotation of the Sun can be explained as rotationally influenced turbulence in the convective zone. The turbulence leads to the formation of large-scale turbulent fluxes (Rüdiger and Hollerbach, 2004). The angular momentum fluxes are proportional to the velocity correlation tensor and are given by:

$$q_{ij} = \overline{v_i' v_j'} \tag{1}$$

where $q_{ij}$ is Reynolds stress tensor, $\boldsymbol{v}$ is velocity, the overbar denotes azimuthal averaging, and primes denote variations about the averages. The latitudinal flux of the angular momentum is described by the horizontal component of the Reynolds stress tensor $q_{\lambda b}$, which can be calculated as the covariance of the meridional motion and the rotation velocity residuals. The rotation and meridional circulation of tracers can easily be determined separately. Therefore, contrary to meridional flow analysis, tracers are suitable tool for analyzing the latitudinal flux of the angular momentum, *i.e.* the turbulent Reynolds stress as the main driver of differential rotation.

Kanzelhöhe Observatory for Solar and Environmental Research (KSO) was founded during WWII as one station within a network of observatories for observing "solar eruptions" (flares) which were interfering with radio communications. Nowadays KSO is affiliated with the University of Graz and performs regular high-cadence full-disk observations of the Sun in the H$\alpha$, the Ca II K spectral lines, and in white light with a coverage of about 300 observing days *per* year (Veronig and Pötzi, 2016).

KSO white light images and sunspot drawings have been used by different authors for measuring the photospheric velocity fields. The data before 1985 were used, *e.g.* by Lustig (1983), Hanslmeier and Lustig (1986), Lustig and Hanslmeier (1987), Balthasar and Fangmeier (1988) and Lustig and Wöhl (1991). Poljančić *et al.* (2010) and Poljančić *et al.* (2011)

**Table 1** The measures of central tendency and dispersion for meridional motions and rotation rate residuals obtained by interactive and automatic methods. Prior to calculation the outliers were discarded. Stdev stands for standard deviation, IQR for interquartile range, Skew for skewness and Kurt for kurtosis.

| Quantity | Method | N | Mean | Median | Stdev | IQR | Skew | Kurt |
|---|---|---|---|---|---|---|---|---|
| $v_{\mathrm{mer}}$ ($\mathrm{m\,s^{-1}}$) | interactive | 961 | 2 | −1 | 74 | 83 | 0.08 | 1.7 |
| $v_{\mathrm{mer}}$ ($\mathrm{m\,s^{-1}}$) | automatic | 792 | −1 | −1 | 73 | 57 | −0.12 | 4.2 |
| $\Delta v_{\mathrm{rot}}$ ($\mathrm{m\,s^{-1}}$) | interactive | 961 | 76 | 77 | 167 | 207 | −0.12 | 0.91 |
| $\Delta v_{\mathrm{rot}}$ ($\mathrm{m\,s^{-1}}$) | automatic | 792 | 5 | −6 | 182 | 144 | 0.04 | 1.4 |

compared the GPR, USAF/NOAA, DPD and KSO sunspot databases and found that DPD and KSO data are, in some respect, more accurate than the USAF/NOAA data. Consequently, the venture of determination of the heliographic positions from the sunspot drawings and full disc white light CCD images was undertaken. The procedure and results for solar rotation in the period 1964 – 2016 are presented in Poljančić Beljan *et al.* (2017). Here we present the analysis of meridional motions and Reynolds stress determined from KSO data in the same period 1964 – 2016.

## 2. Data and Analysis

The drawings of the whole Sun are made at KSO using a refractor telescope ($d/f = 110/1650$ mm). Additionally, from 1989 onwards the white light photographs of the whole Sun are made with a refractor telescope ($d/f = 130/1950$ mm), where the photographic camera was replaced with a CCD camera in July 2007. The positions of the sunspot groups were measured by two methods: interactive and automatic. The interactive procedure was applied for data from 1964 to 2008, where the "Sungrabber" software package (Hržina *et al.*, 2007) was used by two independent observers to measure the positions of group centers on the sunspot drawings made at KSO. For the automatic procedure, morphological image processing based on the "STARA" algorithm (Watson and Fletcher, 2011) was used for the determination of the positions of sunspot groups. The automatic method was applied to the data observed with the digital cameras first of which was installed in July 2007. Since the Solar Cycle 23 ended in 2008 to have an homogeneous dataset within the solar cycle only the data during 2009 – 2016 were obtained by the automatic method. A detailed description of both methods and the availability of the data is given in Poljančić Beljan *et al.* (2017).

To check how the two methods compare with each other the drawings of the whole Sun made during 2014 (solar maximum) were measured using Sungrabber. Descriptive statistics of meridional motions and rotation rate residuals calculated using both methods are presented in Table 1.

A dataset of 45914 times and positions of sunspot groups during the period from January 1964 to April 2016 were used to calculate meridional and rotational speeds. For the sunspot groups for which the Central Meridian Distance (CMD) was less than 58°, which corresponds to about 0.85 of the projected solar radius (Balthasar, Vazquez, and Wöhl, 1986), rotation speeds were calculated by division of CMD differences by elapsed time and meridional motions were calculated by division of latitude differences by elapsed time. This resulted in 33817 rotation and meridional velocity values. The obtained synodic rotation velocities were transformed to sidereal ones by the procedure described in Skokić *et al.* (2014). Finally, to account for errors of misclassification and other errors, an iterative fitting method was used, similar to the one used in Sudar *et al.* (2016) and Sudar *et al.* (2017).

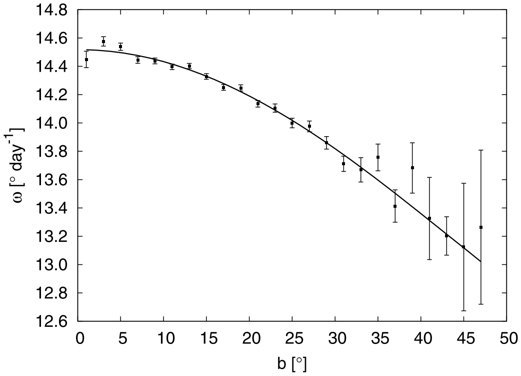

**Figure 1** Differential rotation profile obtained from KSO data from 1964 to 2016. Points with error bars are averaged 2° latitude bin values and the best fit profile (Equation 2) is shown with the *solid line*.

Rotation rate residuals were calculated by subtracting the individual rotation velocities from the average rotation profile:

$$\omega(b) = A + B\sin^2 b, \tag{2}$$

where $A$ and $B$ are differential rotation parameters in [° day$^{-1}$] and $b$ is the heliographic latitude in [°]. Robust statistics of the rotation rate residuals and meridional velocity was used, and values lying outside 3.5 interquartile ranges from the median were considered as outliers and discarded. Since the removed outliers were contributing to the mean rotation profile derived, the process is iteratively repeated until no outliers are present in the data. The procedure converges very fast and after four iterations no outliers were present. Data whose absolute values of rotation rate residual and meridional velocity were larger than 4.2° day$^{-1}$ and 2.3° day$^{-1}$, respectively, were discarded. After applying all these reduction steps 32616 data points are left for further analyses.

In Figure 1 the obtained differential rotation profile is presented, the best fit differential rotation parameters are $A = 14.5177 \pm 0.0096$° day$^{-1}$ and $B = -2.800 \pm 0.088$° day$^{-1}$. The averaged 2° latitude bin values of $\omega(b)$ are also shown. The errors for bins at higher latitudes are quite large due to the small number of sunspots present at these latitudes.

When analyzing latitudinal dependencies the latitude of the first measurement was assigned to each rotational and meridional velocity (Olemskoy and Kitchatinov, 2005) as was done in Sudar *et al.* (2014, 2015, 2016, 2017) to avoid false meridional flows. The rotation rate residuals and meridional velocities were transformed from angular values to linear ones. Taking $R_\odot = 6.96 \times 10^8$ m, the conversion factors are 140.6 and 140.6 $\cos(b)$ m$^{-1}$ day$(°)^{-1}$ for meridional velocities and rotation velocity residuals, respectively, where the latitude of the first measurement was taken into account. In addition, the meridional speeds are transformed so that a negative value of meridional speed represents motion toward the equator for both solar hemispheres. This is achieved by changing the sign of the meridional velocities for the southern solar hemisphere, where negative values of latitude are assigned.

## 3. Results

### 3.1. Latitudinal Dependence of Meridional Motions and Rotation Velocity Residuals

The dependence of meridional motions obtained from the KSO data on latitude is illustrated in Figure 2. The data were averaged over 2.5° in latitude and mean values with error bars are

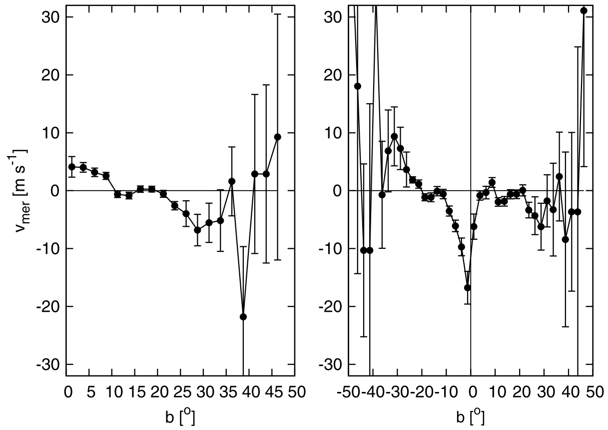

**Figure 2** Meridional motions as a function of latitude. Data are averaged over 2.5° in latitude. In the *left panel* both solar hemispheres are shown together and positive values indicate motion towards the poles. In the *right panel* the northern and southern hemisphere are shown separately and positive values indicate motion towards north.

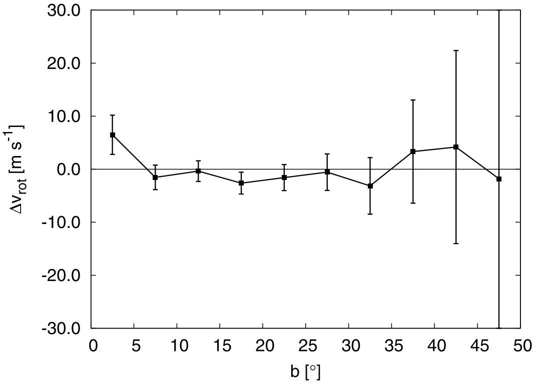

**Figure 3** Rotation velocity residuals as a function of latitude. Data were averaged over 5° in latitude. Positive values denote rotation faster than average and negative values rotation slower than average. The two solar hemispheres have been treated together.

given for each latitude stripe. It can be seen that at low latitudes ($\leq 10°$) meridional motions are toward the poles. The latitude stripes $20° - 30°$ show motions toward the solar equator, while the rest of the values are not significantly different from zero. In the right panel of the figure each solar hemisphere is shown separately. Here the meridional velocities are not transformed and positive values of the meridional velocity denote motion towards north. The result for the southern hemisphere shows motions toward the pole at low latitudes and changes to flow towards north (equator) at higher latitudes. This behavior is reminiscent of that found by Sudar *et al.* (2014) analyzing GPR and USAF/NOAA data and by Sudar *et al.* (2017) studying DPD data. The values for the northern solar hemisphere are not significantly different from zero in all latitude stripes. The most statistically significant values are for stripes $0° - 2.5°$ and $22.5° - 25°$ both showing motions toward south. The observed meridional motions would be consistent with the equatorward motions on the northern solar hemisphere. Such motions were observed on both solar hemispheres by Sivaraman *et al.* (2010) analyzing Kodaikanal and Mt. Wilson data.

Figure 3 shows the dependence of rotation residual velocities on latitude. The data were averaged over 5° in latitude and average values with error bars are presented for each latitude stripe. None of the rotation rate residual values are significantly different from zero.

To examine the changes of meridional circulation with time and the phase of the solar cycle the dataset was divided into four subsets containing individual cycles from Solar Cycle 20 to Solar Cycle 23 and four subsets corresponding to different phases of the cycle. The

**Table 2** Description of data subsets with cycle and phase boundaries. Slope and both intercept values are the result of meridional velocities latitude dependence linear fit. The solar cycle boundaries are taken from Brajša *et al.* (2009).

| Description | Boundaries | Slope | Intercept $Y$ | Intercept $X$ |
|---|---|---|---|---|
| Solar Cycle 20 | 21.10.1964 – 20.04.1976 | −0.42 ± 0.19 | 8.0 ± 2.8 | 19.0 ± 10.0 |
| Solar Cycle 21 | 21.04.1976 – 15.09.1986 | −0.37 ± 0.13 | 4.7 ± 2.2 | 12.7 ± 7.4 |
| Solar Cycle 22 | 16.09.1986 – 25.05.1996 | −0.20 ± 0.11 | 2.1 ± 1.9 | 10.5 ± 11.1 |
| Solar Cycle 23 | 26.05.1996 – 30.06.2008 | −0.43 ± 0.11 | 6.7 ± 1.9 | 15.5 ± 6.0 |
| Minimum from 2y before minimum till 1.5y before maximum | 02.01.1964 – 25.05.1967<br>21.04.1974 – 30.06.1978<br>16.09.1984 – 31.12.1987<br>26.05.1994 – 20.10.1998<br>01.07.2006 – 25.11.2012 | −0.19 ± 0.14 | 3.4 ± 2.5 | 17.9 ± 18.6 |
| Pre maximum from 1.5 y prior to maximum till maximum | 26.05.1967 – 25.11.1968<br>01.07.1978 – 31.12.1979<br>01.01.1988 – 30.06.1989<br>21.10.1998 – 20.04.2000<br>26.11.2012 – 25.05.2014 | −0.45 ± 0.13 | 7.8 ± 2.7 | 17.3 ± 7.8 |
| Past maximum from maximum till 1.5 y after the maximum | 26.11.1968 – 25.05.1970<br>01.01.1980 – 30.06.1981<br>01.07.1989 – 31.12.1990<br>21.04.2000 – 20.10.2001<br>26.05.2014 – 20.04.2016 | −0.33 ± 0.12 | 4.4 ± 2.1 | 13.3 ± 8.0 |
| Declining phase Fom 1.5y after max. till 2y before minimum | 26.05.1970 – 20.04.1974<br>01.07.1981 – 15.09.1984<br>01.01.1991 – 25.05.1994<br>21.10.2001 – 30.06.2006 | −0.45 ± 0.12 | 5.1 ± 1.6 | 11.3 ± 4.7 |

description of the data subsets is given in Table 2. To have sufficient number of data in each latitude stripe both solar hemispheres were treated together and data were averaged over 5° in latitude. The latitudinal dependence of meridional motions for individual solar cycles is presented in the upper row of Figure 4 and the changes within the cycle are shown in the lower row. All meridional velocity profiles show the motions towards the pole at low latitudes and motions towards the equator at higher latitudes. The exception is the profile observed during solar cycle minimum.

The most notable changes are the rise of polarward meridional velocity near the solar equator and the decrease of equatorward velocity at higher latitudes with time. Similar trends can be observed within each solar cycle. However, it should be noted that the changes are not statistically significant due to large errors of the mean velocity near the equator and at higher latitudes due to the smaller number of spots present at these latitudes. In an attempt to quantify the changes of meridional velocity profiles, we calculated linear fits through all datapoints of a given subset. The results of the fit are presented in Table 2. Slope and intercept with both axes are given. All fits have a negative slope which is significant above $2\sigma$ for all solar cycles and all phases of the cycle except the minimum and Solar Cycle 22.

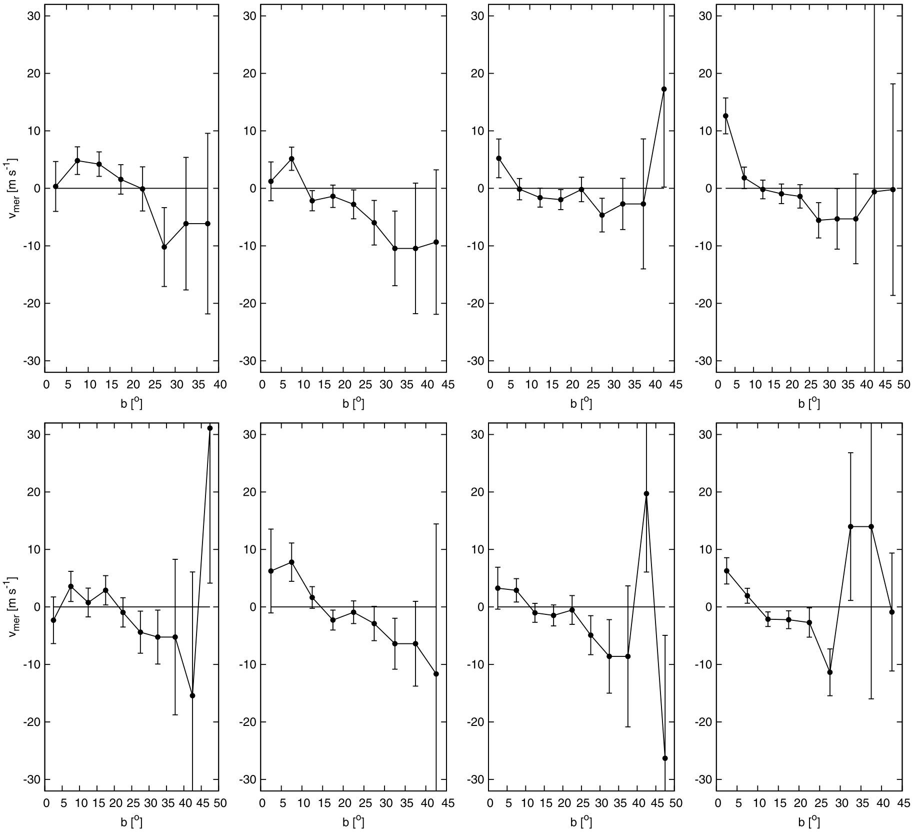

**Figure 4** Meridional motions as a function of latitude. In the *upper row* the profile for each cycle from Solar Cycle 20 to 23 is shown separately (from left to right). In the *lower row* four different phases of the cycle are presented (minimum, pre-maximum, past-maximum and declining phase, from left to right). Velocities belonging to the corresponding phase from all cycles were averaged. Data are averaged over 5° in latitude and both solar hemispheres are shown together to have a sufficient number of data in each latitude bin. Positive values indicate motion towards the poles.

Also, the intercept with the $x$-axis (latitude) decreases with the phase of the cycle, but the change is not statistically significant due to large errors. A similar result was found by Sudar *et al.* (2014).

## 3.2. Correlation Between Meridional Motions and Rotation Rate Residuals and Reynolds Stress

To maintain the observed solar differential rotation profile against diffusive decay, the angular momentum should be somehow transported towards the solar equator. This phenomenon can be observed by investigating the relationship between meridional velocities and rotation velocity residuals. In Figure 5 the meridional velocities are plotted against the rotation rate residuals. The solid line represents the least square fit in the form:

$$v_{\mathrm{mer}} = (-0.0912 \pm 0.0028)\Delta v_{\mathrm{rot}} + (-0.42 \pm 0.43)\ \mathrm{m\,s^{-1}}. \tag{3}$$

**Figure 5** Meridional velocities as a function of rotation rate residuals. Individual data are represented with *points*. The *solid line* is the linear fit (Equation 3).

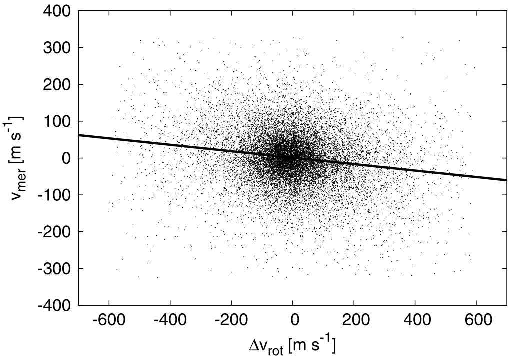

**Figure 6** Horizontal component of the Reynolds stress tensor as a function of latitude. Data were averaged over 10° in latitude. *Solid line* represents best fit in the form of Equation 4. *Shaded areas* are defined by errors of the best fit coefficients (Table 3).

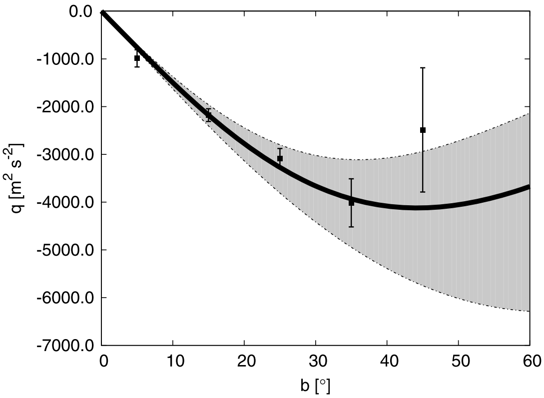

To check for the influence of outliers on the derived parameters in Equation 3 the data were also fitted using least deviation method. The least deviation method gives $-0.088$ and $0.49\ \mathrm{m\,s^{-1}}$ for slope and intercept, respectively.

The slope of the fit is negative indicating that on the average the angular momentum is transported toward the solar equator.

The covariance of meridional velocities and rotation velocity residuals gives the horizontal component of the Reynolds stress tensor. In Figure 6 the horizontal component of the Reynolds stress tensor is shown versus latitude. Values were averaged in 10° latitude stripes. The average values are negative for all latitude stripes which means that the angular momentum is transported towards lower latitudes, *i.e.* toward the solar equator. The solid line in Figure 6 represents the empirical exponential cut-off function (Sudar *et al.*, 2014, 2017) describing the decreasing trend of the horizontal component of the Reynolds stress tensor with latitude:

$$q_{\lambda b}(b) = c_1 b \mathrm{e}^{-c_3 b^2}, \tag{4}$$

where $q_{\lambda b}$ is the horizontal component of the Reynolds stress tensor and $b$ is the latitude. The values of the coefficients $c_1$ and $c_3$ with their respective errors are given in Table 3. The shaded area in the figure is defined by the errors of the coefficients $c_1$ and $c_3$.

**Table 3** Table of the best fit coefficients (Equation 4).

| Coefficient | Value | Relative error |
|---|---|---|
| $c_1$ [$\mathrm{m^2\,s^{-2}\,deg^{-1}}$] | $-154 \pm 11$ | 7.3% |
| $c_3$ [$\mathrm{deg^{-2}}$] | $0.00026 \pm 0.00013$ | 50.8% |

## 4. Discussion and Conclusion

The differential rotation profile obtained in this work is the same (within $1\sigma$) as the one obtained by Poljančić Beljan *et al.* (2017) using the same data and (within $2\sigma$) as by Sudar *et al.* (2017) using the DPD and Sudar *et al.* (2014) using the GPR and USAF/NOAA datasets. The small differences between our result and the result of Poljančić Beljan *et al.* (2017) can be attributed to the different procedures of discarding erroneous values. The iterative procedure applied here results in slightly smaller values for rotation rate than the $8-19^{\circ}\,\mathrm{day}^{-1}$ velocity filter used by Poljančić Beljan *et al.* (2017). The values of differential rotation parameters from different methods and datasets are compared in more detail in Sudar *et al.* (2015) and Poljančić Beljan *et al.* (2017).

The average values of rotation rate residuals which do not differ significantly from zero are indicative of the quality of the solar rotation profile function fit (Equation 2). Further, our results show meridional motions toward the poles at low latitudes and meridional motions toward solar equator at latitudes of $25-30^{\circ}$. This is consistent with the picture of flows directed toward the center of activity (Sudar *et al.*, 2014). Similar results were obtained by Sudar *et al.* (2017) using the DPD dataset. When each solar hemisphere is treated separately, meridional circulation on the southern hemisphere is consistent with flows directed toward the center of activity, while the flows seem to be predominantly equatorward on the northern hemisphere, reminiscent of the flows found by Sivaraman *et al.* (2010) analyzing Kodaikanal and Mt. Wilson datasets. These results confirm that the KSO data are of sufficiently high quality and that they can be used in the analysis of solar velocity patterns.

As summarized in Hathaway (1996) and Sudar *et al.* (2017) the previously obtained results for meridional flows are controversial. Both flows toward and away from the center of activity as well as flows toward the poles and toward the solar equator were observed. Flows out of the center of activity can be attributed to the false assumption that any latitude (latitude of first, last measurement or mean latitude) can be assigned to the observed meridional velocity without taking into account the distribution of tracers. This can result in false flows out of the center of activity (Olemskoy and Kitchatinov, 2005). Next, the cycle dependence of the meridional motions and rotational velocities can influence the results. More detailed explanation of the above-mentioned effects can be found in Sudar *et al.* (2017).

The difference between flows toward the center of activity obtained by sunspot groups and poleward flows shown by Doppler and CBP data can be reconciled if it is assumed that the meridional flow is different in the active regions, where sunspots are located, from the flow outside activity areas (Sudar *et al.*, 2017). Alternatively, the anchoring depth of magnetic features can be important, *i.e.* the differences in velocity patterns measured by different features reflect the differences in the coupling or anchoring depth of those features. Finally, the solar meridional flow might be strongly variable (Hathaway, 1996) and the different results reflect its variability.

When analyzing the meridional motions for possible variations in time and within the solar cycle motions consistent with flows directed toward the center of activity were found. The exception are data for Solar Cycle 22 and the minimum of activity, where the result is more reminiscent of equatorward motions. The minimum of activity dataset contains the sunspot groups belonging to two centers of activity, the one from the preceding cycle at low latitudes and the one from the following cycle at higher latitudes, which can influence the result. Besides, the errors of the meridional velocity values calculated for each latitude stripe for all subsets (not just minimum) are quite large making most of the values statistically insignificant and the most notable changes of the profile are at low latitudes ($< 5^\circ$) and high latitudes ($> 30^\circ$) where the number of data is smallest. Therefore it cannot be concluded that the obtained result represents the actual changes of meridional motions and is not caused by random error of the mean value for given latitude stripe.

By examining the correlation and covariance of meridional velocities and rotation rate residuals we found that the angular momentum is transported towards the solar equator. The horizontal component of the Reynolds stress tensor is found to be in the order of several thousands $\mathrm{m^2\,s^{-2}}$, with the maximal value of $(-4122 \pm 1089)\ \mathrm{m^2\,s^{-2}}$ at $(44 \pm 11)^\circ$ latitude. This is in good agreement with the results of other studies using sunspots as tracers (Ward, 1965; Gilman and Howard, 1984; Pulkkinen and Tuominen, 1998b; Sudar *et al.*, 2014, 2017). This result is also in agreement with the theoretical calculations of Canuto, Minotti, and Schilling (1994), Käpylä *et al.* (2011) and Varela, Strugarek, and Brun (2016). The analysis of the CBP data (Vršnak *et al.*, 2003; Sudar *et al.*, 2016) seems to yield smaller values for the horizontal component of the Reynolds stress. As before, this discrepancy can be reconciled if it is supposed that the Reynolds stress is stronger around active regions. This would imply that the major part of angular momentum transfer occurs in the activity belt. On the other hand, the anchoring depth or height of the tracers might influence the result, too.

By examining the correlation and covariance of meridional velocities and rotation rate residuals it was found that the angular momentum is transported towards the solar equator at all latitudes. Despite meridional motions and rotation rate residuals having values of low statistical significance, their correlation expressed by Reynolds stress is significant, which means that the Reynolds stress is a robust quantity. The absolute value of the horizontal component of Reynolds stress is found to be increasing from the equator attaining maximum at about 40° latitude which is in agreement with results of other studies and theoretical calculations. The observed values of the Reynolds stress are sufficient to maintain the solar differential rotation profile. Therefore, our results confirm that the Reynolds stress is the main contributor to the transport of angular momentum towards solar equator which maintains the observed solar differential rotation. This general result, indicated in various previous studies using other datasets and methods, is now independently confirmed also by using the KSO dataset. The questions of how the anchoring depth of analyzed features and the variability influence the obtained results are still open, and need to be analyzed in the future.

**Acknowledgements** This work was partly supported by the Croatian Science Foundation under the project 6212 “Solar and Stellar Variability” and in part by the University of Rijeka under project number 13.12.1.3.03. We wish to express our gratitude to an anonymous referee, whose careful review and detailed criticism of the manuscript helped to improve the presentation and sharpen the arguments.

**Disclosure of Potential Conflicts of Interest** The authors declare that they have no conflicts of interest.

## References

Balthasar, H., Fangmeier, E.: 1988, Comparison of the differential rotation laws and meridional motions determined from sunspot positions taken from the Greenwich Photoheliographic Results, the drawings of G. Spoerer, and the Kanzelhoehe data. *Astron. Astrophys.* **203**, 381. ADS.

Balthasar, H., Vazquez, M., Wöhl, H.: 1986, Differential rotation of sunspot groups in the period from 1874 through 1976 and changes of the rotation velocity within the solar cycle. *Astron. Astrophys.* **155**, 87. ADS.

Brajša, R., Wöhl, H., Hanslmeier, A., Verbanac, G., Ruždjak, D., Cliver, E., Svalgaard, L., Roth, M.: 2009, On solar cycle predictions and reconstructions. *Astron. Astrophys.* **496**, 855. DOI. ADS.

Brun, A.S., Rempel, M.: 2009, Large scale flows in the solar convection zone. *Space Sci. Rev.* **144**, 151. DOI. ADS.

Canuto, V.M., Minotti, F.O., Schilling, O.: 1994, Differential rotation and turbulent convection: A new Reynolds stress model and comparison with solar data. *Astrophys. J.* **425**, 303. DOI. ADS.

Gilman, P.A., Howard, R.: 1984, On the correlation of longitudinal and latitudinal motions of sunspots. *Solar Phys.* **93**, 171. DOI. ADS.

Haber, D.A., Hindman, B.W., Toomre, J., Thompson, M.J.: 2004, Organized subsurface flows near active regions. *Solar Phys.* **220**, 371. DOI. ADS.

Hanasoge, S., Miesch, M.S., Roth, M., Schou, J., Schüssler, M., Thompson, M.J.: 2015, Solar dynamics, rotation, convection and overshoot. *Space Sci. Rev.* **196**, 79. DOI. ADS.

Hanslmeier, A., Lustig, G.: 1986, Meridional motions of sunspots from 1947.9 – 1985.0. I – Latitude drift at the different solar-cycles. *Astron. Astrophys.* **154**, 227. ADS.

Hathaway, D.H.: 1996, Doppler measurements of the Sun's meridional flow. *Astrophys. J.* **460**, 1027. DOI. ADS.

Howard, R., Gilman, P.I., Gilman, P.A.: 1984, Rotation of the Sun measured from Mount Wilson white-light images. *Astrophys. J.* **283**, 373. DOI. ADS.

Howard, R.F.: 1991, Cycle latitude effects for sunspot groups. *Solar Phys.* **135**, 327. DOI. ADS.

Hržina, D., Roša, D., Hanslmeier, A., Ruždjak, V., Brajša, R.: 2007, Sungrabber – Software for measurements on solar synoptic images. *Central European Astrophysical Bulletin* **31**. ADS.

Käpylä, P.J., Mantere, M.J., Guerrero, G., Brandenburg, A., Chatterjee, P.: 2011, Reynolds stress and heat flux in spherical shell convection. *Astron. Astrophys.* **531**, A162. DOI. ADS.

Lustig, G.: 1983, Solar rotation 1947 – 1981 – Determined from sunspot data. *Astron. Astrophys.* **125**, 355. ADS.

Lustig, G., Hanslmeier, A.: 1987, Meridional motions of sunspots from 1947.9 to 1985.0. II – Latitude motions dependent on SPOT type and phase of the activity cycle. *Astron. Astrophys.* **172**, 332. ADS.

Lustig, G., Wöhl, H.: 1991, The meridional motions of stable recurrent sunspots. *Astron. Astrophys.* **249**, 528. ADS.

Lustig, G., Wöhl, H.: 1994, Meridional motions of sunspot groups during eleven activity cycles. *Solar Phys.* **152**, 221. DOI. ADS.

Mandal, S., Hegde, M., Samanta, T., Hazra, G., Banerjee, D., Ravindra, B.: 2017, Kodaikanal digitized white-light data archive (1921 – 2011): Analysis of various solar cycle features. *Astron. Astrophys.* **601**, A106. DOI. ADS.

Olemskoy, S.V., Kitchatinov, L.L.: 2005, On the determination of meridional flow on the Sun by the method of tracers. *Astron. Lett.* **31**, 706. DOI. ADS.

Poljančić, I., Brajša, R., Ruždjak, D., Hržina, D., Jurdana-Šepić, R., Wöhl, H., Otruba, W.: 2010, A comparison of sunspot position measurements from different data sets. *Sun Geosph.* **5**, 52. ADS.

Poljančić, I., Brajša, R., Hržina, D., Wöhl, H., Hanslmeier, A., Pötzi, W., Baranyi, T., Özgüç, A., Singh, J., Ruždjak, V.: 2011, Differences in heliographic positions and rotation velocities of sunspot groups from various observatories. *Cent. Eur. Astrophys. Bull.* **35**, 59. ADS.

Poljančić Beljan, I., Jurdana-Šepić, R., Brajša, R., Sudar, D., Ruždjak, D., Hržina, D., Pötzi, W., Hanslmeier, A., Veronig, A., Skokić, I., Wöhl, H.: 2017, Solar differential rotation in the period 1964-2016 determined by the Kanzelhöhe data set. *Astron. Astrophys.* **606**, A72. DOI. ADS.

Pulkkinen, P., Tuominen, I.: 1998a, Velocity structures from sunspot statistics in cycles 10 to 22. I. Rotational velocity. *Astron. Astrophys.* **332**, 748. ADS.

Pulkkinen, P., Tuominen, I.: 1998b, Velocity structures from sunspot statistics in cycles 10 to 22. II. Latitudinal velocity and correlation functions. *Astron. Astrophys.* **332**, 755. ADS.

Rüdiger, G., Hollerbach, R.: 2004, *The Magnetic Universe: Geophysical and Astrophysical Dynamo Theory*, 343. ADS.

Ruždjak, D., Ruždjak, V., Brajša, R., Wöhl, H.: 2004, Deceleration of the rotational velocities of sunspot groups during their evolution. *Solar Phys.* **221**, 225. DOI. ADS.

Sivaraman, K.R., Sivaraman, H., Gupta, S.S., Howard, R.F.: 2010, Return meridional flow in the convection zone from latitudinal motions of umbrae of sunspot groups. *Solar Phys.* **266**, 247. DOI. ADS.

Skokić, I., Brajša, R., Roša, D., Hržina, D., Wöhl, H.: 2014, Validity of the relations between the synodic and sidereal rotation velocities of the Sun. *Solar Phys.* **289**, 1471. DOI. ADS.

Sudar, D., Skokić, I., Ruždjak, D., Brajša, R., Wöhl, H.: 2014, Tracing sunspot groups to determine angular momentum transfer on the Sun. *Mon. Not. Roy. Astron. Soc.* **439**, 2377. DOI. ADS.

Sudar, D., Skokić, I., Brajša, R., Saar, S.H.: 2015, Steps towards a high precision solar rotation profile: Results from SDO/AIA coronal bright point data. *Astron. Astrophys.* **575**, A63. DOI. ADS.

Sudar, D., Saar, S.H., Skokić, I., Poljančić Beljan, I., Brajša, R.: 2016, Meridional motions and Reynolds stress from SDO/AIA coronal bright points data. *Astron. Astrophys.* **587**, A29. DOI. ADS.

Sudar, D., Brajša, R., Skokić, I., Poljančić Beljan, I., Wöhl, H.: 2017, Meridional motion and Reynolds stress from Debrecen Photoheliographic Data. *Solar Phys.* **292**, 86. DOI. ADS.

Švanda, M., Kosovichev, A.G., Zhao, J.: 2008, Effects of solar active regions on meridional flows. *Astrophys. J. Lett.* **680**, L161. DOI. ADS.

Varela, J., Strugarek, A., Brun, A.S.: 2016, Characterizing the feedback of magnetic field on the differential rotation of solar-like stars. *Adv. Space Res.* **58**, 1507. DOI. ADS.

Veronig, A.M., Pötzi, W.: 2016, Ground-based observations of the solar sources of space weather. In: Dorotovic, I., Fischer, C.E., Temmer, M. (eds.) *Coimbra Solar Physics Meeting: Ground-Based Solar Observations in the Space Instrumentation Era*, *Astronomical Society of the Pacific Conference Series* **504**, 247. ADS.

Vršnak, B., Brajša, R., Wöhl, H., Ruždjak, V., Clette, F., Hochedez, J.-F.: 2003, Properties of the solar velocity field indicated by motions of coronal bright points. *Astron. Astrophys.* **404**, 1117. DOI. ADS.

Ward, F.: 1965, The general circulation of the solar atmosphere and the maintenance of the equatorial acceleration. *Astrophys. J.* **141**, 534. DOI. ADS.

Watson, F., Fletcher, L.: 2011, Automated sunspot detection and the evolution of sunspot magnetic fields during solar cycle 23. In: Prasad Choudhary, D., Strassmeier, K.G. (eds.) *Physics of Sun and Star Spots*, *IAU Symposium* **273**, 51. DOI. ADS.

Wöhl, H., Brajša, R.: 2001, Meridional motions of stable recurrent sunspot groups. *Solar Phys.* **198**, 57. DOI. ADS.

Zuccarello, F., Zappalá, R.A.: 2003, Angular velocity during the cycle deduced using the sunspot group age selection methodology. *Astron. Nachr.* **324**, 464. DOI. ADS.